コンクリート工学年次論文報告集，Vol. 18, No. 2, 1996

論文 Evaluation of Fracture Energy of Early Age Concrete by a Non-Local Plasticity Model

Khan Mahmud Amanat*, Tada-aki Tanabe**

ABSTRACT: A non-local plasticity [1,2] model is used to investigate the effect and applicability of using different forms of gradient parameter on localization phenomena and on fracture energy consumed. It was found that the form of gradient influence factor significantly influences the formation of localization band and the consumption of fracture energy. Based on the results an approximate analytical expression is proposed to calculate the fracture energy when the gradient term is chosen independently. Finally some experimental results are simulated to show how the values of different material parameters can be selected.
KEY WORDS: Localization, Non-local, Strain Softening, Fracture Energy, Gradient Plasticity.

1 INTRODUCTION

Fracture of concrete is a highly localized phenomenon where failure is induced by concrete cracking principally in mode-I type crack and the post-peak load response decreases sharply with increasing deformation. Study [3] shows that in the fracture process zone stress does not drop suddenly, instead, it follows a progressive strain softening due to non-homogeneous deformations resulting from macroscopic cracking [4]. It shows some ductility, because the faces of cracks are connected by grain bridges which delay crack propagation and opening [4]. Recognizing the strain softening characteristics of the fracture process of concrete it is possible to simulate the same in the domain of continuum mechanics. Application of classical plasticity can be applied but it has few major drawbacks -- the result is mesh sensitive, fracture process zone cannot propagate beyond those area defined explicitly beforehand, strain field between the boundary of fracture process zone and elastic zone is discontinuous, and the ellipticity of the governing differential equation is lost in the post peak regime. These drawbacks can be overcome by the use of enhanced continuum approaches like the integral approach [5] or gradient plasticity approach [1,2]. In this study the gradient approach has been adopted to simulate the fracture process of early age concrete.

The study presented here is a continuation of the work done earlier by the authors [6,7]. The gradient plasticity formulation contains one important parameter g which is called the gradient influence factor. The gradient influence factor g governs the extension and growth of localization zone. As it will be shown later, g affects the final load-displacement response of the structure, thus affecting the fracture energy consumed by the structure. Hence it is necessary to incorporate the influence of g in fracture energy calculation. In this study this parameter is studied in details and an approximate analytical expression is suggested to calculate the fracture energy. Finally using a proposed softening rule analysis was performed to simulate the fracture process of concrete at early ages.

2 MATERIAL MODEL

In gradient plasticity [1] approach the Laplacian of the damage parameter, κ, is incorporated in the failure function. Thus the failure condition reads as,

$$f\left(\sigma, \kappa, \nabla^2 \kappa\right) = 0 \tag{1}$$

* Graduate Student, Dept. of Civil Engineering, Nagoya University, Japan. Member , JCI
** Professor, Dept. of Civil Engineering, Nagoya University, Japan. Member, JCI

It is imperative that for simple one dimensional case, κ can be directly set equal to the plastic strain and for two dimensional case it can be a direct function of plastic strain components $d\varepsilon_{ij}^{p}$. Setting $\dot{f}=0$ we get the flow consistency condition (from eq.1),

$$\frac{\partial f}{\partial \sigma}d\sigma+\frac{\partial f}{\partial \kappa}d\kappa+\frac{\partial f}{\partial \nabla^2\kappa}\nabla^2(d\kappa)=0 \tag{2}$$

Assuming that the damage parameter κ is related to the plastic multiplier λ as $\dot{\kappa}=\eta\dot{\lambda}$ where η is a positive constant and using the notations,

$$\mathbf{n}=\frac{\partial f}{\partial \sigma} \quad , \quad h=\frac{\partial f}{\partial \kappa} \quad , \quad g=\eta\frac{\partial f}{\partial \nabla^2\kappa} \tag{3}$$

we get the plastic flow consistency equation from eq. (2),

$$\mathbf{n}^{\mathrm{T}}\dot{\sigma}-h\dot{\lambda}+g\nabla^2\dot{\lambda}=0 \tag{4}$$

As a result of the presence of the term $\nabla^2\lambda$, it is not possible to solve for λ directly from eq.(4). Hence in gradient plasticity λ is solved globally by making it a global unknown [1]. In this paper it is considered that g is a function of damage κ only. The failure function in eq. (1) has the form,

$$f(\sigma,\kappa,\nabla^2\kappa)=\varphi(\sigma)-\bar{\sigma}_g(\kappa,\nabla^2\kappa) \tag{5}$$

where φ(σ) is a function of stress components (usually stress invariants) and σ_g is the yield strength which depends on both κ and $\nabla^2\kappa$. For one-dimensional case φ(σ) is simply the axial stress σ . In two dimensional analysis φ(σ) may take various form such as Rankine's principal stress criteria or Von Mises criteria etc. In this paper, fracture of early age concrete in simple tension is studied and Rankine's principal stress criteria of failure is adopted. Thus,

$$\varphi(\sigma)=\sigma_m=\frac{1}{2}\left(\sigma_x+\sigma_y\right)+\frac{1}{2}\sqrt{\left(\sigma_x+\sigma_y\right)^2+4\tau_{xy}^2} \tag{6}$$

In $(\sigma_x,\sigma_y,\tau_{xy})$ stress space Rankine failure function possesses a vertex at $(\bar{\sigma},\bar{\sigma},0)$ point. The existence of this vertex poses some difficulties in return mapping algorithm. In classical plasticity approach this difficulty can be overcome by assuming each smooth part of the failure function as a separate function and then applying Koiter's generalizations. In gradient plasticity this approach is not suitable because λ is also a global variable like the displacement field. An alternate approach is to smoothen the failure function in the vertex regime [8]. In this approach the Rankine square shaped failure surface in tension-tension regime is replaced by a smooth circular one. When this is done, the failure function takes the form,

$$f=\sqrt{(\sigma_1^2+\sigma_2^2)}-\bar{\sigma}_g=\sqrt{(\sigma_x^2+\sigma_y^2+\tau_{xy}^2)}-\bar{\sigma}_g=0 \tag{7}$$

However, an incompatibility exists along the σ_x and σ_y axis in the stress space. Therefore this smoothing approach is will be made active when stress state will be dominated by tension and not by shear.

3 GRADIENT INFLUENCE FACTOR AND CALCULATION OF FRACTURE ENERGY

The form gradient dependent yield strength, $\bar{\sigma}_g$, adopted in this paper is,

$$\bar{\sigma}_g=\bar{\sigma}_t(\kappa)-g(\kappa)\nabla^2\kappa \tag{8}$$

where $\bar{\sigma}_t(\kappa)$ is a given standard softening rule and $g(\kappa)$ is a given gradient influence function. As it is seen from eq.(6) the degradation of yield strength depends on $g(k)$ as well as on $\bar{\sigma}_t(\kappa)$. Hence it is logical that the load displacement response or the fracture energy consumed will be governed, in part, by the gradient influence factor $g(k)$ and thus, the selection of the form of $g(\kappa)$ is an important consideration in gradient plasticity formulation. For a one dimensional problem with linear softening (softening modulus h constant) and constant g Borst [1] obtained a relation,

$$g=-l^2\sigma_t'(\kappa)=-l^2h \tag{9}$$

where l is the internal length scale such that the crack band width is given by

$$w=2\pi l \tag{10}$$

When the softening rule $\bar{\sigma}_t(\kappa)$ is nonlinear and g is taken according to the first part of eq. (9) then eq. (10) becomes approximate. An exact analytical solution for such a case is a mathematically formidable task. In all the previous studies with gradient plasticity approach, $g(\kappa)$ has always been taken according to eq. (9) so that the width of the fracture process zone can be estimated by eq. (10). If the width of the fracture process zone, w, is known then the fracture energy is given by,

Table 1. Softening rule

Description	Figure
Non-linear softening, $\bar{\sigma}_t(\kappa) = \frac{f_t}{c_1+1}\left[c_1 e^{-c_2 \kappa/\kappa_u} + \left(1 - \frac{\kappa}{\kappa_u}\right)\right]$ c_1=10, c_2=6	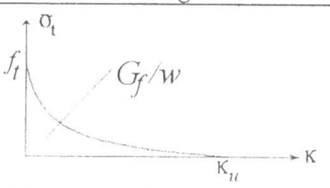

Table 2. Different forms of $g(\kappa)$

Type	Description	Figure
g1	*Constant:* $g(\kappa) = c_5 l^2 \frac{f_t}{\kappa_u}$ c_5=0.9c_2	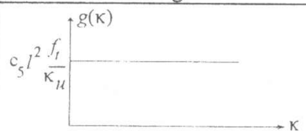
g2	*Linearly decreasing:* $g(\kappa) = c_3 f_t l^2 \left(1 - \frac{\kappa}{\kappa_u}\right)$ c_3=900	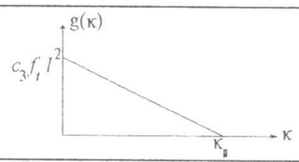
g3	*Non-linear:* $g(\kappa) = c_3 f_t\, e^{-c_4 \kappa}$ c_3=900, c_4=500	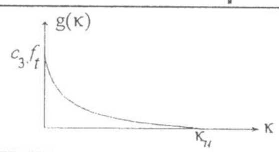
g4	*Proportional to* $\bar{\sigma}_t'(\kappa)$: $g(\kappa) = \frac{f_t l^2}{c_1+1}\left(c_1 c_2 e^{-c_2 \frac{\kappa}{\kappa_u}} + \frac{1}{\kappa_u}\right)$	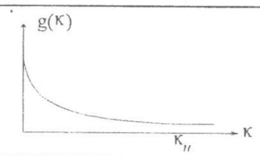

$$G_f = w \int_0^{\kappa_u} \bar{\sigma}_t(\kappa) d\kappa \tag{11}$$

where κ_u is the ultimate value of damage parameter at which $\bar{\sigma}_t(\kappa)$ becomes zero. Equation (11) is valid only when w is constant and can be approximated by eq. (10), i.e., when g is taken according to eq. (9). However, the basic formulation of gradient plasticity does not impose such limitation on the form of $g(\kappa)$. In this paper several forms of $g(\kappa)$ are considered to study how different forms of $g(\kappa)$ influences the post peak response. Table 1 lists the softening function and table 2 lists the different forms of $g(\kappa)$ which are considered in this paper.

When $g(\kappa)$ is chosen independently of eq.(9) it is also necessary to develop an appropriate expression for fracture energy since eq.(11) remains no longer valid. In this study it is assumed that the actual value of internal length scale varies according to the values of $g(\kappa)$ and $\bar{\sigma}_t'(\kappa)$ at any stage of damage but maintains the basic form of eq.(9). Thus,

$$l = l(\kappa) = \sqrt{-\frac{g(\kappa)}{\bar{\sigma}_t'(\kappa)}} \tag{12}$$

Now eq.(11) is modified by taking w inside the integral and substituting $2\pi l(\kappa)$ for w,

$$G_{fg} = 2\pi \int_0^{\kappa_u} l(\kappa)\, \bar{\sigma}_t(\kappa) d\kappa \tag{13}$$

In such a case the term l in the different expressions in table 2 merely becomes a material parameter rather than the actual internal length scale.

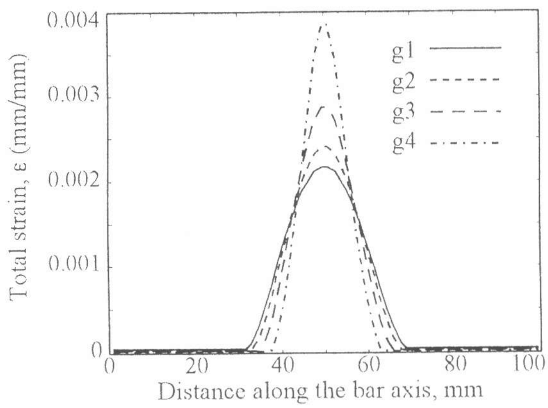

Fig.1 Strain distribution along the bar axis

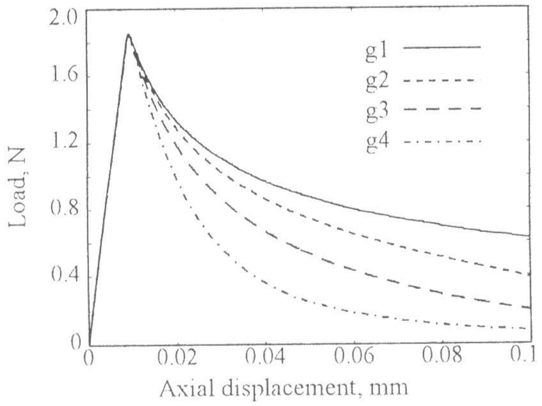

Fig.2 Load-displacement response

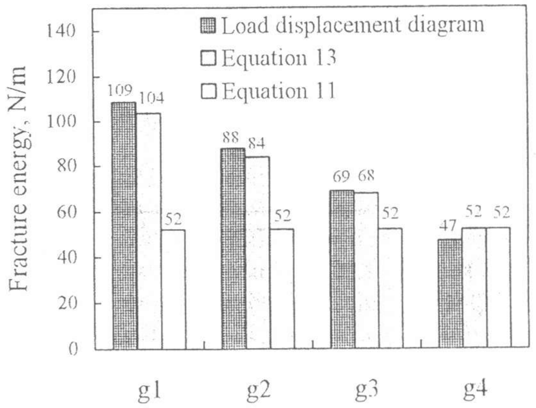

Fig.3 Fracture energy calculated by different methods.

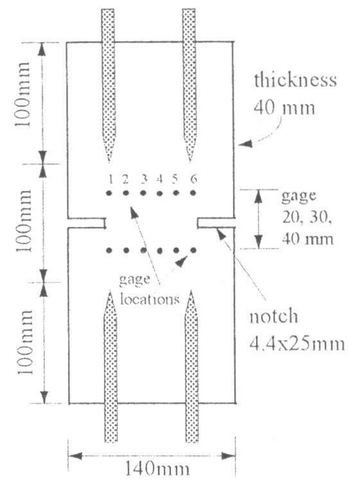

Fig.4 Test specimen

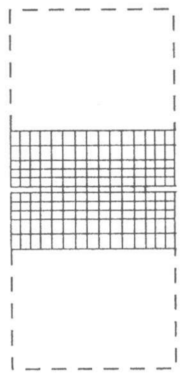

Fig.5 FEM mesh.

4 NUMERICAL STUDY

A rigorous numerical study was made in one dimension with different combinations of softening rule and gradient influence factor. For the purpose of study a bar under uniaxial tension is considered. The length of the bar is L = 100 mm with a unit cross sectional area. The initial values of other parameters are, modulus of elasticity $E = 20000$ N/mm^2, tensile strength $f_t = 2$ N/mm^2, internal length scale $l = 4$ mm. For the softening rule, ultimate value of equivalent fracture strain was $\kappa_u = 0.006$. The results correspond to a mesh size of 30 elements with a relatively denser mesh at central region. Three noded gradient enhanced elements were used with quadratic shape functions for displacement field and cubic Hermitian shape functions for λ. To trigger localization at the center of the bar only two elements at the center of the bar (covering approximately 3.2 mm length at center) were made weak by reducing tensile strength by 10%. However, as the amount of plastic strain increases during loading process more and more adjacent elements entered into localization process due to gradient effect until a steady state condition was reached finally.

Fig.1 shows the strain distribution obtained for different types of $g(\kappa)$. It is seen that different forms of $g(\kappa)$ resulted in different amount of damage growth. The width of the fracture localization zone were also different for different types of $g(\kappa)$. The load-displacement diagram obtained for different $g(\kappa)$ is shown in fig.2. Since in each case the area under the load-displacement diagram is different, the fracture energy is also different for each case. If the fracture energy is calculated using eq.(11) by taking $w \approx 2\pi l$ it will give same fracture energy value for all the cases since $\bar{\sigma}_t(\kappa)$ is same for all the cases. The energy

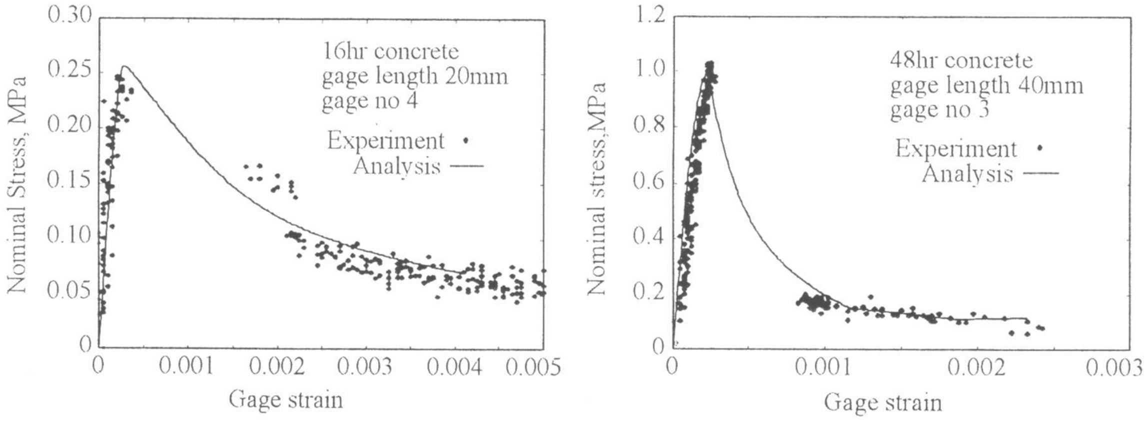

Fig.6 Comparison of numerically and experimentally obtained stress strain relations

Table 3 Material parameters

Age	E, MPa	ν	c_1	c_2	κ_u	f_t, MPa	l, mm
16 hour	1000	0.15	2.0	5.5	0.02	0.25	2.0
48 hour	8000	0.15	2.0	5.5	0.011	1.1	1.3

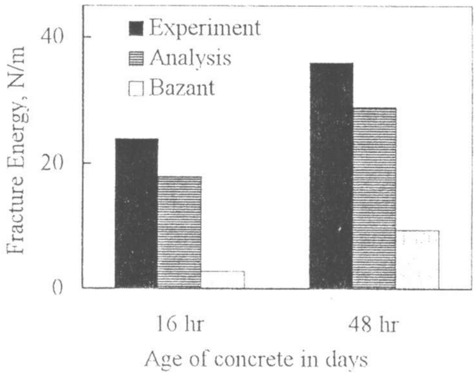

Fig.7 Comparison of fracture energy obtained by different method

calculated from the area under the load-displacement curve is the actual energy consumed. This energy can be analytically estimated by using the eq.(13) this should agree with the value calculated from the load displacement response. A look a fig.3 reveals that the energy given by eq.(11) gives unacceptable values for the first three types of $g(\kappa)$. On the other hand, the energy calculated by eq.(13) and the same calculated form load displacement response agrees well. The small differences observed between these two process is due to the assumption made in eq.(12). Actually $l(\kappa)$ follows a more complex route with the change of damage and its exact analytical formulation is mathematically formidable. However, the accuracy of eq.(12) and eq.(13) are well enough for all practical purposes as revealed from fig.3. Thus, the proposed equations (12) and (13) enables us to take any reasonable form of $g(\kappa)$ instead of taking it as $-l^2\bar{\sigma}_t'(\kappa)$ as done in the previous works [1,6,7,8].

5 ANALYSIS OF EXPERIMENTS

In the next stage of this study the two-dimensional formulation was applied to simulate test results [9] on early age concrete. For this purpose the fracture condition of eq.(7) was adopted. Test were made on concrete specimens at ages 9, 16, 24, 48, 72 and 102 hours. Due to the space limitation results for only the specimens of age 16 hour and 48 hour are shown here. The original specimen was 300mm long, 140mm wide and 40mm thick and had a pair of notch having dimensions 4.4mm×25mm. A pair of 18mm diameter steel rods were embedded longitudinally at each end of the specimen to facilitate loading. The length of the embedded rods were 100mm. Due to the presence of these rods the outer 100mm portions at both end of the specimen were rather stiff compared to the central 100mm portion. At early age both the stiffness and the strength of concrete are very low. So it is quite reasonable to assume that for young age concrete, the two ends having embedded rod elements will behave almost rigidly as compared to the central portion. Based on such assumption when the test specimen was discretized into finite elements, higher stiffness values were assigned to these two 100mm outer portion. Also another finite element mesh was considered which represented only the central 100mm portion. After making some preliminary analysis, it was observed that both types of mesh discretization give virtually the same result when high stiffness was assigned to the 100mm portions at the ends in the former type of mesh. But the second type of mesh was computationally more efficient since it required less number of elements. Hence the later type of discretization was adopted finally for the numerical analysis and the mesh is shown in fig.5.

The values of different material parameters that were taken for the numerical simulations are shown in table 3. The Young's modulus was calculated from the initial slope of the stress strain curve obtained experimentally and an averaging was done over the values calculated from each of the six strain-gages (gages 1 to 6). Due to the lack of experimental data, Poisson's ratio was taken as 0.15. Other values such as κ_u etc. are taken in such a way that the numerical results best fits the experimental data. Analysis was performed with *g(k)* as *g4*.

The fracture energy was calculated by Lokuliyana [9] from the experimentally obtained stress strain relation. A comparison of the calculated values with the Bazant's [10] equation was also made. Figure 7 summarizes the fracture energy calculated by the different methods. It is observed that the G_f calculated in according to eq.(13) are somewhat smaller than the experimental values. The results are on the safe side and may be considered acceptable since the difference is not too large as compared with the G_f calculated using Bazant's formula which gives too small fracture energy to be considered acceptable.

6 CONCLUSION

The form of the gradient influence factor has significant effect on the overall post-peak response of the structure and on development of the fracture process zone. A modified way of calculating the fracture energy is presented in the context of simulating fracture and localization of concrete structures by gradient plasticity approach. Incorporation of the variable internal length scale parameter inside the integral of the fracture energy expression enables us to use any reasonable shape of the gradient influence factor while resulting approximately correct value of fracture energy.

A softening function is presented to describe the strength degradation of early age concrete. A two dimensional analysis is performed and it has been shown that using the proposed softening rule the fracture process of concrete at early age can be simulated and its fracture energy can be evaluated with reasonable accuracy.

REFERENCES

[1] Borst R. de, and Mühlhaus H. B.: Gradient-Dependent Plasticity: Formulation and Algorithmic Aspects, *Int. J. Num. Meth. Eng.*, Vol. 35, pp. 521-639, 1992.

[2] Mühlhaus H. B. and Aifantis E.C.: A Variational Principle for Gradient Plasticity, *Int. J. Solids Structures*, Vol. 28, pp. 845-857, 1991.

[3] Read, H.E. and Hegemier, G.A.: Strain Softening of Rock, Soil and Concrete - a Review Article, *Mechnanics of Materials Journal*, Vol. 3, pp.271-294, 1984

[4] Mier, J.G.M. van: Mode-I Fracture of Concrete: Discontinuous Crack Growth and Crack Interface Grain Bridging, *Cement and Concrete Research*, Vol. 21, pp.1-15, 1991

[5] Bazant, Z.P. and Pijaudier-Cabot, G.: Non-local Continuum Damage, Localization Instability and Convergence, *Journal of Applied Mechanics*, Vol. 55, pp.287-293, 1988.

[6] Amanat K.M. and Tanabe T: Numerical Study on Fracture Process of Concrete by Gradient Plasticity Models, *Proc. of International Symposium on NewDevelopment in Concrete Science and Technology*, Southeast University, Nanjing, China, Sept., 1995.

[7] Amanat K.M. and Tanabe T: Applicability of One Dimensional Gradient Plasticity in Identifying Fracture Process of Concrete, *Proc. of JCI*, Vol. 17, 1995.

[8] Pamin, J.: *Gradient-Dependent Plasticity in Numerical Simulation of Localization Phenomena*, PhD Thesis, Department of Civil Engineering, Delft University of Technology, Netherlands, 1994.

[9] Lokuliyana, D.R., Tanabe, T: *Fracture Mechanics Based Analysis of Thermal Crack Propagation of massive Concrete*, NUCE Research Report No. 9202, Dept. of Civil Engineering, Nagoya University, Japan, July 1992.

[10] Bazant, Z.P.: Mechanics of Fracture and Progressive Cracking in Concrete Structures, *Chap. 1, Fracture mechanics of Concrete: Structural Application and Numerical Calculation*, edited by Sih, G.C. and DiTommaso, A., Martinus Nijhoff Publishers, 1985.